

DOI: ADD DOINUMBER HERE

Multirow flutter in low pressure turbines: Comparison of different blade configurations

Oscar Bermejo*, Juan Manuel Gallardo*, Adrian Sotillo Ramos* and Carlos Augusto Diaz†

*Department of Simulation Technology

Industria de Turbo Propulsores S.A.U., 28108, Alcobendas, Madrid, Spain

†Department of Mechanical Technology

Industria de Turbo Propulsores S.A.U., 48170, Zamudio, Vizcaya, Spain

oscar.bermejo@itpaero.com · juan.gallardo@itpaero.com · adrian.sotillo@itpaero.com · carlos.diaz@itpaero.com

Abstract

The focus of this paper is to study and compare the multirow effects on the aerodynamic damping of a low pressure turbine blade for different mechanical configurations. For this purpose, a traditional cantilevered blade and a “welded-in-pairs” assembly have been chosen, using the same blade geometry in both cases. The methodology used is based on the transmission of spinning modes between rows and relies on ITP’s in house linear CFD code. Those spinning modes will be decomposed into acoustic and convective terms and the individual contribution of each wave to the global damping will be analyzed.

Nomenclature

AR	Aspect Ratio
c	Blade chord
CFD	Computational Fluid Dynamics
$c_{m,n}$	Acoustic mode amplitude
IBPA	Inter-blade phase angle
k	Scatter index
k_x	Axial wave number
LPT	Low Pressure Turbine
m	Circumferential wave number
MTO	Maximum Takeoff
N_b	Number of blades
ND	Nodal Diameter
NRBC	Non reflecting boundary conditions
R_0	Vibrating rotor
S_{-1}	Upstream stator
S_1	Downstream stator
\tilde{U}	Unsteady perturbations of primitive variables
\hat{U}	Circumferential Fourier transform of unsteady perturbations of primitive variables
$v_{m,n}^L$	Left eigenvector
$u_{m,n}^+$	Downstream acoustic modes (right eigenvector)
$u_{m,n}^-$	Upstream acoustic modes (right eigenvector)
V_{out}	Velocity modulus at outlet
ξ	Critical damping ratio
ω	Vibrational frequency
Ω	Rotational speed

MULTIROW FLUTTER

1. Introduction

For the last decades there has been a steady trend to design high lift, highly loaded low pressure turbines (LPTs) with slender, high aspect-ratio airfoils. This leads to a reduction in weight and cost, and a potential increase in efficiency, but also has negative consequences: the stiffness of the bladed-disk assembly tends to decrease, and its natural frequencies with it. In practice, the susceptibility of an assembly to aeroelastic issues, particularly flutter, increases as the frequency decreases; this imposes significant constraints to the design space. This issue has been addressed by developing different configurations with increased stiffness and/or improved aeroelastic behaviour.

When considering shrouded turbine blades, the most straight-forward configuration is cantilever (figure 1), with flat-sided shrouds with a clearance between them. This imposes no restrictions to the blade vibrations, which makes the configuration noticeably flutter-prone. A widely spread solution involves z-shaped shrouds (interlocks, figure 1), which are designed to remain tightly in contact during the whole flight envelope. Interlocked blades show remarkably different dynamic characteristics from their cantilever counterparts, including higher natural frequencies, a strong dependence on the nodal diameter, and significant coupling between bending and torsion modes. However, this very complex behaviour, which is exacerbated once in-service conditions and wear are taken into account, is a serious drawback.

Another alternative configuration involves welding the (flat) shrouds of pairs of adjacent blades (also shown in figure 1). This has a moderate impact on the natural frequencies, while the mode-shapes remain conceptually similar to the cantilevered blade, but with the additional constraint that the pairs of blades move in phase.

A detailed comparison of the flutter behaviour of these three configurations (cantilever, interlock and welded-in-pair) was presented in [1]. There, it was shown that the stabilizing effect of the welded-in-pair configuration was much larger than what the small frequency increase and (seemingly) moderate effect in mode-shape suggested. Nevertheless, it must be highlighted that the conclusions in that work were sustained by single row unsteady CFD simulations, which were consistent with the industry standard at the time.

On the other hand, the effect of multi-row interactions in turbomachinery aeroelasticity is a topic which has received a remarkable degree of attention in the last decade, with works like [2], [3], [4] or [5] presenting numerical methods able to analyzing these interactions with different degree of generality. Other authors, such as Zhao et al. [6] have focused their effort in explaining the physics behind these interaction mechanisms. The stabilizing effect of multi-row interaction in low pressure turbine flutter was studied in [7] and [8], using a welded-pair configuration as the focus of the analysis. In the current work, the aim is to compare the flutter behaviour of cantilever and welded-in-pair turbine blades, while using the methodology described in [7] to include the multi-row interactions.

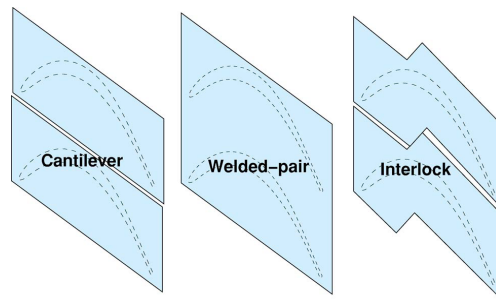


Figure 1: Different blade shroud attachments

2. Multirow methodology**2.1 Code description**

The simulations described here are based on the in-house CFD solver suite Mu^2s^2T developed at ITP. This code solves the 3D RANS equations using hybrid unstructured grids to discretize the spatial domain and stores the solution at cell vertex points. Two schemes can be chosen to perform the time integration, namely a fully implicit Jacobi solver or an explicit five-stage Runge Kutta scheme. Turbulence modeling options include Wilcox's two equation $k-\omega$ and algebraic Baldwin-Lomax eddy viscosity models. More details can be found at [9, 10, 11, 12].

The time linearized solver $Mu^2s^2T - L$ included in the suite has been used to run the unsteady flutter computations presented in this work. Consistency between the linear and non-linear solvers is guaranteed as they share common data structures and analogous algorithms are employed when possible. Its capabilities for the determination of flutter [13, 1] and turbine tonal noise propagation [14, 15, 16] have been thoroughly validated.

Multirow unsteady simulations performed in our study involve multiple linearized solutions, each one associated to a different frequency, that coexist at any particular blade-row of the simulation domain, all of them coupled with the solutions lying in the neighbor blade-rows. This is possible thanks to the coupling mechanism implemented in our linearized solver.

2.2 Spinning modes theory

The fundamental idea behind the multirow coupling methodology is that the whole unsteady flow field can be transferred without modification in inter-row boundaries, allowing acoustic, vorticity and entropy perturbations to propagate through the entire flow domain.

The unsteady solution must be decomposed into Fourier modes in circumferential direction, which take the name of spinning modes or traveling waves. That is the form that better matches the formulation of the coupling methodology. These modes can be expressed as:

$$\tilde{U}(x, r, \theta, t) = \sum_m \hat{U}_m(x, r) e^{-i\omega_0 t + im\theta} \quad (1)$$

where

$$\hat{U}_m(x, r) = \frac{1}{P} \int_P \tilde{U}(x, r, \theta) e^{-im\theta} d\theta \quad (2)$$

For this kind of simulations in cylindrical ducts, phase-shift boundary conditions are a ubiquitous feature. That imposes an important limitation to what circumferential modes could exist:

$$m_k = M + k \cdot N_B, \quad k \in \mathbb{Z} \quad (3)$$

In theory, the scatter index k can take an infinite number of values, leading to an unlimited number of spinning modes interacting between them. However, only a few of them contribute in practice to the unsteady flow field solution coupled between rows.

Another aspect of the coupling mechanism that is worth mentioning is the frequency shift that any of these spinning modes will undergo when the reference frame changes. This is a direct consequence of the Doppler effect. The following equation expresses the relation between frequencies in that case:

$$\omega_1 + m_k \Omega_1 = \omega_2 + m_k \Omega_2 \quad (4)$$

2.3 Acoustic analysis

The unsteady flow field associated to any spinning mode can be further decomposed into its physical components. To do that, we should perform a generalized eigenvalue analysis of the linearized 3D Navier-Stokes equations, considering that we have small unsteady perturbations over the mean flow, which is axially and circumferentially uniform, but varies radially. The eigenmodes of such an analysis take the form:

$$\tilde{U}(x, r, \theta, t) = u(r) e^{-i\omega_0 t + im\theta + ik_x x} \quad (5)$$

As a result of this analysis, we obtain a set of eigenvalues $k_{x,m,n}$ with a right eigenmode ($u_{m,n}(r)$) and a left eigenmode ($v_{m,n}(r)$) associated to each one of them. Letter n represents here a radial index for each mode.

For a detailed description of the whole process, the interested reader should refer to [17].

The complete set of eigenvalues and eigenmodes resulting from this analysis should be divided in acoustic modes, which will carry the vast majority of the pressure perturbation, and nearly-convected waves, which are dominated by vorticity and entropy. However, as Golubev et al. stated in their work [18], the nearly-convected waves cannot be accurately described with this normal mode analysis, so we will not use them in the breakdown of the unsteady flow field.

Each acoustic mode has an associated amplitude which is obtained as the inner product of the left eigenmode and the unsteady flow field:

$$c_{m,n} = \langle v_{m,n}^L \cdot \hat{U}_m \rangle \quad (6)$$

Thus, the complete acoustic field can be described as:

$$\hat{U}_{A,m}(x, r) = \sum_n c_{m,n}^+ u_{m,n}^+(r) e^{ik_{x,m,n}^+ x} + \sum_n c_{m,n}^- u_{m,n}^-(r) e^{ik_{x,m,n}^- x} \quad (7)$$

MULTIROW FLUTTER

where acoustic modes are divided in downstream (+) and upstream (-) moving modes.

Finally, as we know that the complete unsteady flow field is the sum of acoustic and nearly-convected fields: $\hat{U}_m(x, r) = \hat{U}_{A,m}(x, r) + \hat{U}_{C,m}(x, r)$, the nearly-convected field $\hat{U}_{C,m}$ can be obtained just by a simple subtraction.

The numerical value of $k_{x,m,n}$ determines the physical condition for the propagation of acoustic modes:

- when k_x is a pure real number, that means the wave propagates with no attenuation. This kind of waves are called 'cut-on' waves.
- when k_x is a complex number, that means the wave decays exponentially as it propagates. This kind of waves are called 'cut-off' waves.

This eigenvalue analysis will greatly improve our capabilities to research into what are the most important physical aspects of the multirow interaction in flutter simulations, by being able to independently evaluate the effect of different circumferential and radial acoustic modes as well as the impact of nearly-convected perturbations in the coupled unsteady solution.

2.4 Non-reflecting boundary conditions

The acoustic analysis performed in the previous section is also useful for the development of a 3D unsteady non-reflecting boundary conditions scheme. For that purpose, we should consider the fact that apart from any externally imposed perturbation, the unsteady flow field in any inflow or outflow boundary should only consist of outgoing perturbations. Furthermore, as the number of spinning modes considered in any simulation is limited, these boundary conditions will also be applied in inter-row boundaries to those spinning modes that will not be transferred to the neighbor domain.

The iterative scheme implemented in the solver to enforce them is:

$$\begin{aligned}\hat{U}_{m,inlet} &= \sum_n \left(\langle v_{m,n}^{L,-} \cdot \hat{U}_m \rangle u_{m,n}^- \right) \\ \hat{U}_{m,outlet} &= \hat{U}_m - \sum_n \left(\langle v_{m,n}^{L,-} \cdot \hat{U}_m \rangle u_{m,n}^- \right)\end{aligned}\quad (8)$$

following the strategy explained by the work of Moinier et al. [19].

3. Test case description

The model of study is representative of the final stages of modern low pressure turbines (LPT). The selected blade geometry presents a very high aspect ratio ($AR \approx 8.6$), which makes the configuration noticeably flutter prone. In the next sections we will analyze the flutter stability of the blade row considering two different assemblies, namely cantilever and welded-in-pairs configurations. The cantilever configuration entails 156 blades with their root attached to the disk with fir-trees and with free tip displacements, working as cantilever beams. On the other hand, the welded-in-pairs arrangement involves 78 pairs of blades which have been welded through the shroud adding a degree of restriction to the tip displacements; the attachment of those pairs to the disk remains unchanged.

Although the airfoil geometry used is exactly the same in both cases, the different mechanical arrangements lead to different modal properties. Typically, for the cantilever configuration the first three modal families correspond to flap (bending perpendicular to chord), edgewise (bending parallel to chord) and torsion modes. Figure 2 shows the modal shapes for our cantilevered airfoil. The flap and torsion modes are consistent with this simplified description, but the edgewise mode presents a non-negligible torsion component in this case.

The welded-in-pairs modes can be observed in figure 3. The flap mode is very similar to the one found in the cantilever case, the main difference being that no inter-blade phase angle appears in the motion between the two blades forming the pair. The second mode corresponds to a edge-torsion mode with the torsion center located in one of the blades. That blade will follow a torsion motion meanwhile the other will move mainly edgewise. Finally, the third mode corresponds to a classical torsion mode with the torsion center located between both blades.

If we take a look at the reduced frequencies of our problem in figure 4, the first thing we observe is that the values are very small (below 0.25 in all cases), thus it is very likely that our modes will be unstable to flutter. The second thing is that frequencies change from one configuration to the other. The welded in pairs adds rigidity to the flap mode and the frequency rises about 17% when compared to the cantilever. No significant changes appear in the second family frequencies (the welded shroud is not effective when restricting edgewise displacements), and finally the torsion mode becomes more flexible for the welded configuration, with lower frequency than the cantilever.

The flutter stability of the assemblies was determined at Maximum Take-Off (MTO) conditions. The mesh used in the analysis has about 2 million nodes per passage and row, with 95 radial planes and roughly 80 points per wavelength

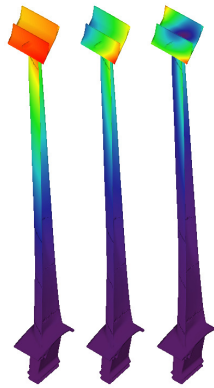


Figure 2: Modal shapes for cantilever configuration. Modes 1 to 3 from left to right.



Figure 3: Modal shapes for welded in pairs configuration. Modes 1 to 3 from left to right.

for the highest circumferential mode considered, which leads to negligible numerical dissipation. We would like to remark that the mesh used in the welded-in-pairs study has been generated by duplicating the mesh of the cantilever case so that the comparison of the results is as fair as possible.

Two kind of analyses will be presented in the following sections, that is, single row and multirow analysis. In the single row study the blade is treated as an isolated row imposing 3D nrbc at inlet and outlet, so that no physical or numerical reflections exist. In the multirow analysis, the vibrating blade and the two adjacent stators (115 vanes in each stator row) are considered. Also, three spinning modes will be transmitted between rows (the fundamental mode m_0 plus the modes $m_{\pm 1}$) and 3D nrbc will be applied at our domain limits (inlet of the first vane and outlet of the last vane). Circumferential modes $m_{\pm 2}$ will also be treated with 3D nrbc at the inter row boundaries. Following the results presented in [7], this setting should capture the majority of the physics involved in the problem.

4. Single row analysis

A common way to determine the flutter stability is to compute the aerodynamic damping curves. These curves represent the aerodynamic damping of a given family mode against the inter-blade phase angle, that is, the phase between the displacements of two adjacent blades (or adjacent pairs of blades, when considering the welded-in-pair configuration). According to our sign criteria a negative damping value means that energy is being transferred from the air flow to the blade, thus the motion is unstable.

The results obtained from the isolated row simulation show our blade is unstable for both configurations and for the first three modal families, as we can see in figure 6. This is not surprising given the very high aspect ratio of the

MULTIROW FLUTTER

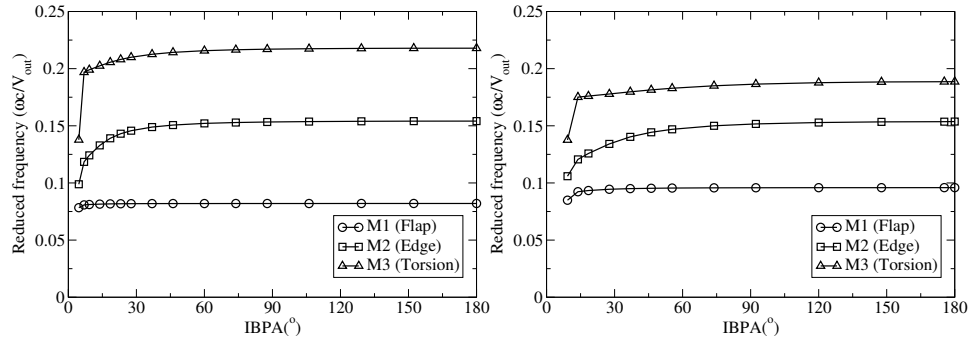


Figure 4: Reduced frequencies for the first three modes of cantilever (left) and welded in pairs (right) configurations.

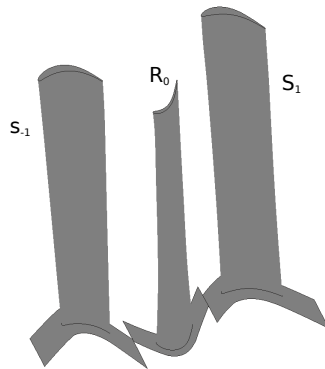


Figure 5: Schematics of studied rows and nomenclature.

selected geometry, which leads to very low reduced frequencies, as shown in figure 4.

The other conclusion we can obtain from this analysis is that the welded in pairs configuration shows a noticeably lower instability than its cantilever counterpart. The main reason behind that behavior can be found in the shape modes resulting from both assemblies. As no inter-blade phase angle acts between the two blades of the same pair, the unsteady pressure levels generated in that region tend to be low. Therefore, the region with pressure levels capable of producing significant work reduces in the welded in pairs configuration when compared to the cantilever. More details about this can be found in [1].

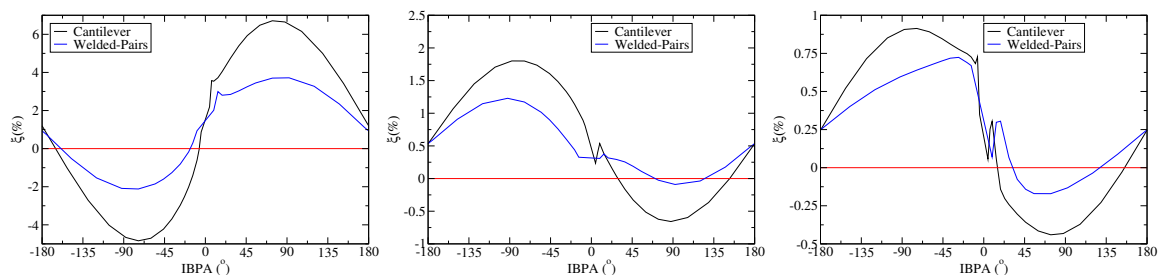


Figure 6: Aerodynamic damping curves for flap (left), edge (center) and torsion (right) modes. Single row analysis

5. Multirow analysis

In typical turbomachinery, blade rows are not isolated and operate in the presence of more rows. Perturbation waves generated by the vibrating blade travel upstream and downstream reaching other rows, reflecting and eventually coming back to the vibrating blade, modifying the unsteady pressure field and as a result the aerodynamic damping. For that reason, a multirow analysis is of interest.

Figure 7 compares the damping curves obtained in the isolated row and multirow analysis. The first thing we should notice is that the reflections play a very significant role in the stability determination. Also it is important to realize that

the effect of the reflection is of the same nature for both configurations (stabilization for modes 1 and 3, destabilization for mode 2), but with different intensity. We would like to highlight the third (torsion) mode, where reflections produce a complete stabilization of the welded in pairs configuration.

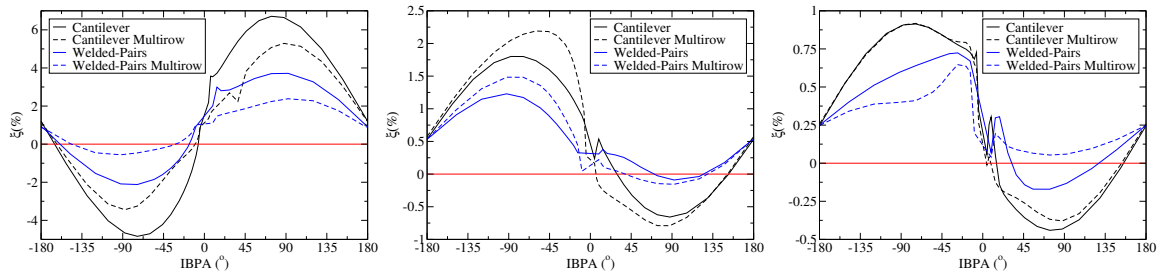


Figure 7: Aerodynamic damping curves for flap (left), edge (center) and torsion (right) modes. Multirow analysis

In the next sections we will present a detailed study of the unstable region of each modal family. The unsteady flow field associated to the vibrational problem is very complex so a further decomposition of the solution is needed. We have defined a number of constant axial coordinate sections where the field will be decomposed into its acoustic and convective modes. We can see in figure 8 an example of the unsteady pressure modulus at midspan for one of the flutter cases analyzed in this work. Notice the study sections depicted in the plot.

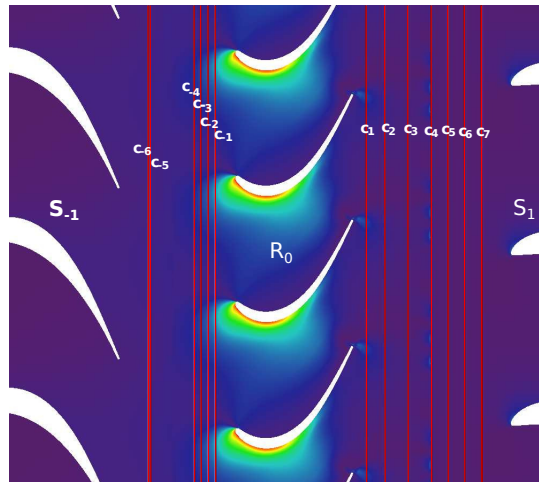


Figure 8: Modulus of the unsteady pressure for $ND=-32$, cantilever configuration. Notice the study sections marked.

5.1 First modal family (flap)

Multirow interactions have an stabilizing effect for this modal family in both configurations. However, the strength of this effect is larger in the welded in pairs model, specially in relative terms (instability is reduced by 30% for the cantilever case and by 70% for the welded-in-pairs assembly). To explain that difference a deeper analysis of the region with most unstable inter-blade phase angles should be taken.

As we mentioned before in section 2 the interaction between rows happens through spinning modes that travel between them. The first thing we should notice is that the spinning modes generated by each configuration are different. On one hand the most unstable nodal diameter (which corresponds to $IBPA = -73.84^\circ$) is $ND = -32$ for the cantilever configuration and $ND = -16$ for the welded in pairs, so the fundamental mode ($m_0 = ND$) differs in both cases. On the other hand the number of units of interest also differs (156 cantilever blades against 78 welded pairs). Taking into account the equation 3, we can find that the spinning modes generated by the cantilever configuration are $m_0 = -32$, $m_1 = 124$ and $m_{-1} = -188$, whereas the welded in pairs assembly will generate the modes $m_0 = -16$, $m_1 = 62$ and $m_{-1} = -94$.

The cut-off ratio of the acoustic modes of each spinning mode depends strongly on its mode number. Higher mode numbers tend to increase cut-off ratios, thus making the acoustic part of the problem decay faster. In this study case, spinning mode numbers are higher for the cantilever geometry and as a result the decay ratio of the acoustics waves

MULTIROW FLUTTER

will be higher for that configuration. This is confirmed by the fluid eigenvalues shown in Figure 9. Remember that the cut-off ratio corresponds to the imaginary part of those eigenvalues.

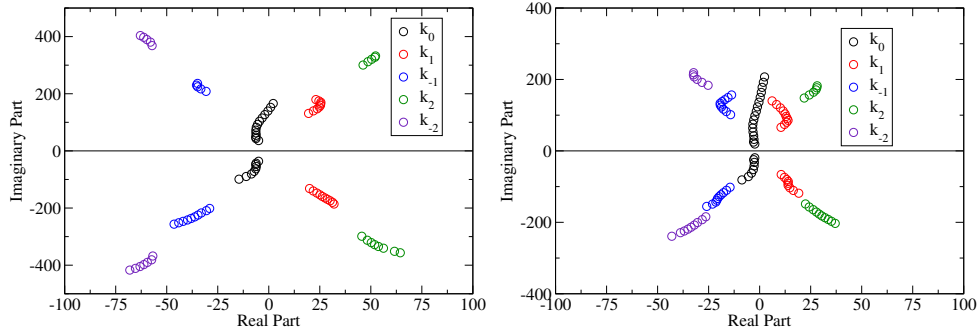


Figure 9: Fluid eigenvalues for cantilever (left) and welded in pairs (right) configurations.

It is important to highlight that the multirow effect is strong even though no cut-on acoustic modes appear in the problem. This means that the rows are close enough for the waves to travel between them without completely disappearing. Figure 10 shows the evolution of the amplitude of the generated acoustic modes on their way from the vibrating blade to the neighboring vanes and compares it with the theoretical decay according to their cut-off ratio. The first two acoustic radial modes from the decomposition of each spinning mode are shown. We can observe that the pressure levels of the generated waves are comparable in both configurations. This is not surprising as the modal shape is similar in both cases (a flap mode). Given that the generated wave amplitudes are similar in both cases, the acoustic waves reaching the neighbor rows will be weaker in the cantilever configuration due to their higher decay ratio.

However, acoustic waves are just part of the physics as convective terms play a non-negligible role in the problem. These waves have no decay and only propagate downstream. For that reason, when analyzing their individual effect we have to take into account that they will only cover the gap between rows once, and the other half of the journey will be covered by the corresponding acoustic wave. Thus, cut-off ratios may also affect their final impact although to a lesser extent than in the pure acoustic contributions.

The total multirow effect has been decomposed in four different components according to their nature (for the sake of simplicity, only the main circumferential mode m_0 will be analyzed as the vast majority of the physics are associated to that mode). These components are the pure acoustic and convective interactions with S_{-1} and S_1 . Please note that the two convective interactions have slightly different nature in each case. Regarding S_{-1} the convective waves are result of the reflection of the acoustic waves that travel upstream from the blade, meanwhile in S_1 the convective waves are generated by the blade and the final interaction is produced by acoustic modes that come back from the vane as a result of the reflection. Figure 11 shows that decomposition for m_0 . We can see that the principal contributor to the aerodynamic damping is the convective wave coming from S_{-1} with a non negligible contribution from the acoustic waves coming from S_1 . As expected, the acoustic waves are more relevant in the welded in pairs configuration but the same can not be said for the convective perturbations, which produce similar damping in both cases, although slightly higher in the cantilever. The sum of all contributions gives similar values for the two configurations, a little bit higher

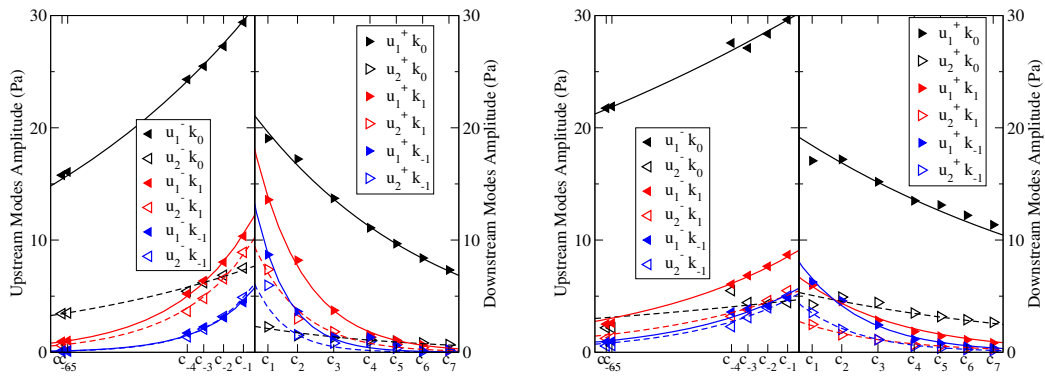


Figure 10: Evolution of acoustic waves generated by flap mode of the cantilever (left) and welded in pairs (right) configurations. Sub index number indicates the radial mode. Super index indicates the wave traveling direction: upstream (-) and downstream (+)

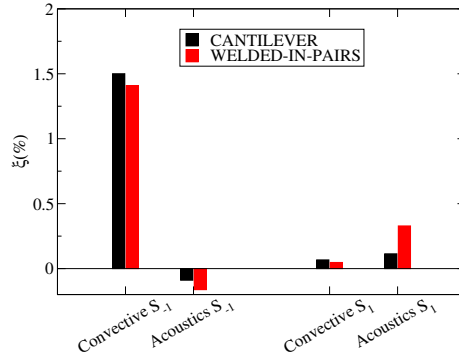


Figure 11: Individual damping deltas produced by convective and acoustic waves interaction with S_{-1} and S_1 for flap mode.

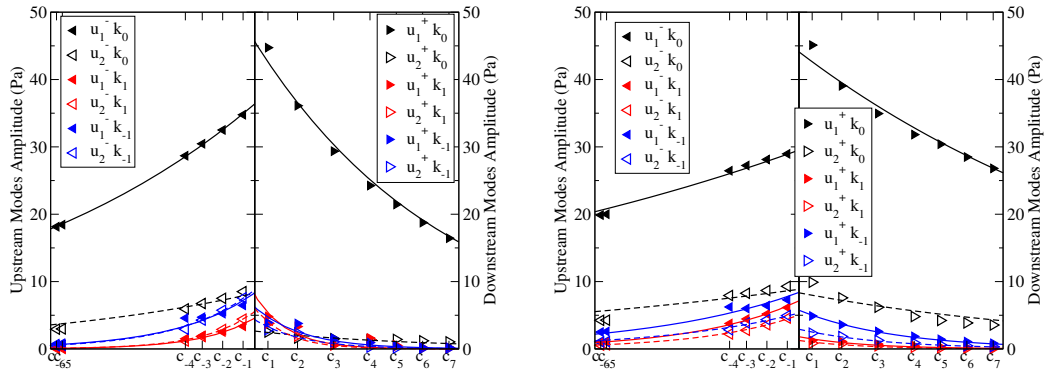


Figure 12: Evolution of acoustic waves generated by edge mode of the cantilever (left) and welded in pairs (right) configurations. Sub index number indicates the radial mode. Super index indicates the wave traveling direction: upstream (-) and downstream (+)

in the welded in pairs thanks to the stronger acoustics. However, as we can see in figure 6, the cantilever was very unstable when analyzed as an isolated row, thus the effect of the multirow interactions remains weaker in relative terms.

5.2 Second modal family (edge)

In this case, multirow interactions have a negative impact on flutter stability as the multirow simulation gives us a more negative aerodynamic damping value than the corresponding isolated row simulation (see figure 7, central graph). As we did with the flap mode, a further analysis of the unstable region will be shown in this section. For this mode, the unstable region is located at positive IBPA. We will study the $IBPA = 73.84^\circ$ point, which corresponds to nodal diameters 32 and 16 for the cantilever and welded pairs configurations respectively. This leads to the circumferential modes $m_0 = 32$, $m_1 = 188$ and $m_{-1} = -124$ for the cantilever, and modes $m_0 = 16$, $m_1 = 94$ and $m_{-1} = -62$ for the welded in pairs. Once again, the spinning modes involved in the problem are higher for the cantilever, thus the associated decay ratio of the acoustic terms will also be higher for that configuration.

Generated acoustic waves have similar amplitudes in both configurations, the upstream modes being slightly stronger in the cantilever. However, this difference is not enough to counteract the effect of the decay ratio. Downstream acoustic modes have larger amplitude than upstream modes, thus the interaction with S_1 should have a moderately larger relative weight than in the flap mode case.

If we split the multirow effect of circumferential mode m_0 into its different components as we did for the flap mode, we can see that the unstabilizing effect, which is dominant, comes from the convective interaction with S_{-1} , meanwhile the main stabilizing effect is produced by the acoustic interaction with S_1 . The latter is specially significant for the welded in pairs configuration and is able to partially offset the unstabilizing impact of the convective waves coming from S_{-1} , thus reducing the final damping delta.

It might be surprising the fact that the convective interaction with S_{-1} is clearly stronger in the welded option despite the fact that convective waves have similar amplitude in both cases (the acoustics reaching S_{-1} are similar in both cases and the reflected waves are comparable). We have to keep in mind that regarding this family mode, unlike

MULTIROW FLUTTER

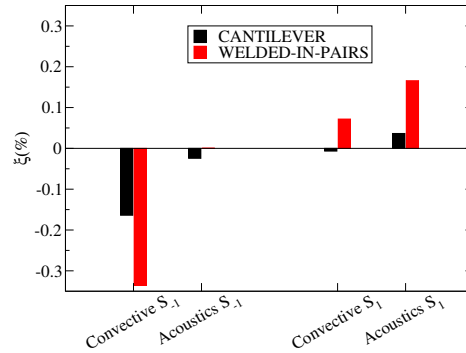


Figure 13: Individual damping deltas produced by convective and acoustic waves interaction with S_{-1} and S_1 for edge mode.

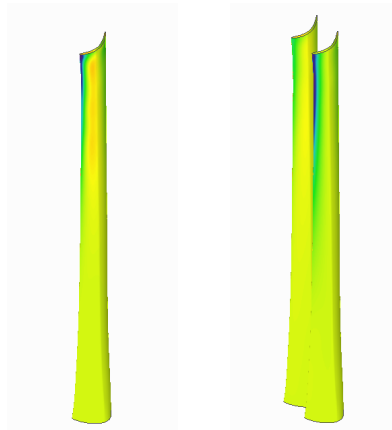


Figure 14: Work distribution produced by convective waves coming from S_{-1} for second modal family in the cantilever (left) and welded in pairs (right) configurations.

flap mode, modal shapes are quite different for both configurations. Taking a look to figures 2 and 3, we can see that this particular edge mode has a clear torsion component. In the welded-in-pairs assembly the blade closer to the torsion center will have similar modal shape to the cantilever blade, meanwhile the other blade will present a stronger edge component. Figure 14 shows the work distribution produced by the convective waves coming from the upstream vane in both cases. Unsurprisingly, the leading edge concentrates most of the activity in both configurations. The key fact here is that in the welded-in-pairs assembly the blade that produces the vast majority of the negative work is the one whose modal shape differs from the cantilever mode. Then, we can affirm that the stronger unstabilizing effect in the welded blades comes from their modal shape rather than from the nature of the reflected waves.

Finally we would like to mention that although all contributions are individually stronger in the welded in pairs option, the global effect is similar for both configurations due to the different sign of each term. This result might be misleading and suggest that reflections have the same impact in both configurations, when actually they are more intense in the welded-in-pairs assembly. The relative weight of each contribution varies from case to case and leads to a different global effect.

5.3 Third modal family (torsion)

Multirow effects produce a stabilization of the torsion mode for both configurations, as we can see in figure 7 (right), but the effect is really strong in the welded in pairs configuration where a complete stabilization occurs.

A further analysis of the unstable region shows some interesting things. The selected point for that study is the same as in mode 2, that is $IBPA = 73.84^\circ$, that corresponds to $ND = 32$ for the cantilevered blade and $ND = 16$ for the welded pair. The circumferential mode numbers that come into play here are exactly the same than in the edge mode. So, as it happened for previous modal families, acoustics will decay faster for the cantilever than for the welded in pairs configuration.

Taking a look at figure 15 we can see a couple of things. First, the acoustic perturbations generated by the welded-

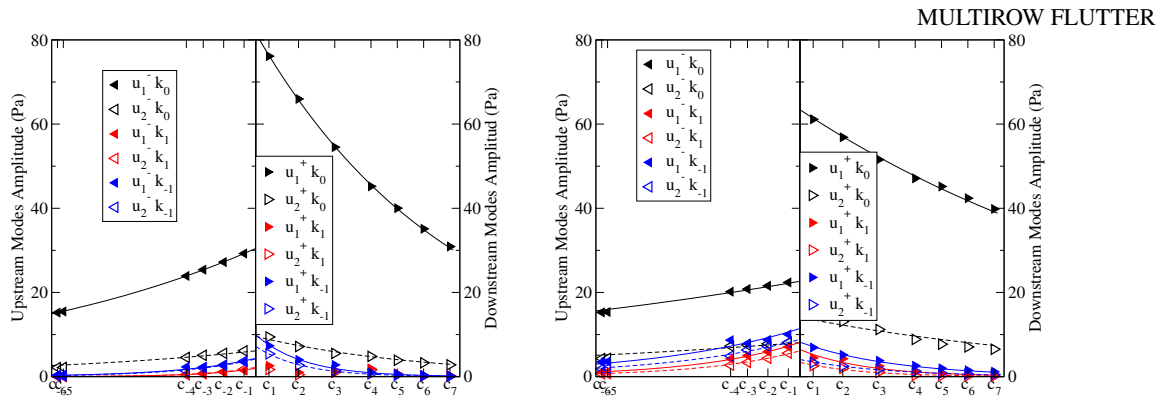


Figure 15: Evolution of acoustic waves generated by torsion mode of the cantilever (left) and welded in pairs (right) configurations. Sub index number indicates the radial mode. Super index indicates the wave traveling direction: upstream (-) and downstream (+)

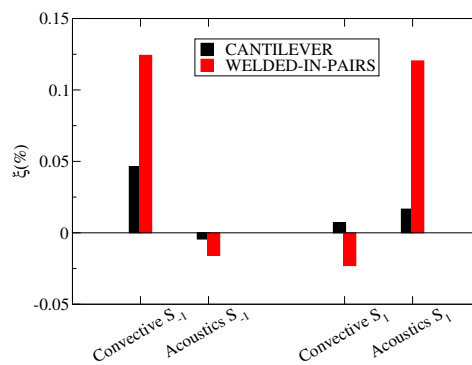


Figure 16: Individual damping deltas produced by the interaction of m_0 convective and acoustic terms with S_{-1} and S_1 for torsion modal family.

in-pairs arrangement are weaker than those generated by the cantilever case, but thanks to their lower decay ratio they maintain a higher amplitude when reaching S_{-1} and S_1 . If we take into account the propagation of the acoustic modes back to the vibrating blades, we can determine that acoustics will have a much deeper impact on damping in the welded option. Second, acoustic modes going downstream are clearly stronger than those traveling upstream, thus we can expect that the contribution of the downstream reflections to the damping will gain relative weight. Remember that for previous modes the dominant effect was the convective term coming from S_{-1} .

The previous reasoning is confirmed by the results. Taking a look at figure 16 we discover that the convective waves resulting from S_{-1} reflection are still dominant, but the acoustics coming from S_1 have a comparable impact for the welded-in-pairs configuration. In the cantilever case this is not happening because of the high decay of its acoustic waves. Once again, all the terms produce more damping in the welded in pairs, including the convective waves coming from S_{-1} . This could be surprising if we consider that the amplitude of these waves is not so very different in both cases (as we can see in figure 15 acoustics reaching the upstream vane have similar intensity in both cases, and the reflection coefficient does not change so much between both problems). And once again, as it happened with the second mode, we must find the explanation in the modal shapes.

Although both configurations exhibit a torsion modal shape, the torsion axis is not located at the same point. For the cantilevered blade, the torsion axis is placed in the middle of the blade meanwhile in the welded in pairs configuration it falls somewhere between both blades. Thus, each blade will follow a motion which is different from that followed by the cantilever. We know that the stability of torsion modes is very sensitive to the position of the torsion center, so we can expect variations in the damping values obtained (see [1]). Moreover, in this case some of the displacement components are in opposite phase for the two blades forming the pair. Thus, the phasing between the displacements and the unsteady pressure, which is essential to determine the damping will differ from blade to blade in the welded arrangement, and from configuration to configuration too.

Finally, we would like to add that in this case, unlike what happened in the second mode, the two main contributions have the same sign, and therefore the higher individual impact found in the welded arrangement directly turns into a higher global impact.

MULTIROW FLUTTER

6. Conclusions

The multirow effect on the aerodynamic damping of a LPT blade is studied via the simulations presented in this paper. A state-of-the-art methodology has been developed at ITP to include these effects in our flutter assessment.

The two proposed configurations, namely cantilever and welded-in-pairs, have been studied and the latter has been found significantly more stable from the flutter point of view. This effect is present when analyzing in isolation the vibrating row, but is further magnified when taking multirow interactions into account. The main difference between both assemblies, regarding multirow interaction, resides on the higher decay of the acoustic waves in the cantilever case that reduces their impact on the aerodynamic damping.

7. Acknowledgments

The authors wish to thank “Industria de Turbo Propulsores S. A. U.” for allowing the publication of this paper.

References

- [1] Roque Corral, Juan Manuel Gallardo, and Carlos Vasco. Aeroelastic stability of welded-in-pair low pressure turbine rotor blades: A comparative study using linear methods. *Journal of Turbomachinery-transactions of The Asme - J TURBOMACH-T ASME*, 129, Jan 2007.
- [2] K.C. Hall, K. Ekici, and D.M. Voytovych. chapter Multistage Coupling for Unsteady Flows in Turbomachinery. *Unsteady Aerodynamics, Aeroacoustics and Aeroelasticity of Turbomachines*. Springer, Dordrecht, 2006.
- [3] Gabriel Saiz. *Turbomachinery Aeorelasticity using a Time-Linearised Multi Blade-row Approach*. PhD thesis, Imperial College, 2008.
- [4] M. T. Rahmati, L. He, and R. G. Wells. Interface treatment for harmonic solution in multi-row aeromechanic analysis, 2010.
- [5] Kwen Hsu, Dan Hoyniak, and M. S. Anand. Full-annulus multi-row flutter analyses, 2012.
- [6] Fanzhou Zhao, Jens Nipkau, and Mehdi Vahdati. Influence of acoustic reflections on flutter stability of an embedded blade row. *Proceedings of the Institution of Mechanical Engineers, Part A: Journal of Power and Energy*, 230(1):29–43, 2016.
- [7] Adrian Sotillo and Juan Manuel Gallardo. Study of the impact of multi-row interaction on flutter analysis for a representative lpt geometry, 2018.
- [8] Juan Manuel Gallardo, Adrián Sotillo, and Óscar Bermejo. Study of the effect of the scatter of acoustic modes on turbine flutter. *Journal of Turbomachinery*, pages 1–22, May 2019.
- [9] Roque Corral, Javier Crespo, and Fernando Gisbert. chapter Parallel Multigrid Unstructured Method for the Solution of the Navier-Stokes Equations. *Aerospace Sciences Meetings*. American Institute of Aeronautics and Astronautics, Jan 2004.
- [10] Fernando Gisbert, Roque Corral, and Jesus Pueblas. chapter Computation of Turbomachinery Flows with a Parallel Unstructured Mesh Navier-Stokes equations Solver on GPUs. *Fluid Dynamics and Co-located Conferences*. American Institute of Aeronautics and Astronautics, Jun 2013.
- [11] Jesus Pueblas, Roque Corral, and Fernando Gisbert. chapter Selection of Implicit CFD Techniques for Unstructured Grids and Turbomachinery Applications. *Fluid Dynamics and Co-located Conferences*. American Institute of Aeronautics and Astronautics, Jun 2013.
- [12] Javier Crespo, Roque Corral, and Jesus Pueblas. An implicit harmonic balance method in graphics processing units for oscillating blades. *Journal of Turbomachinery*, 138(3):031001–031001–10, Nov 2015.
- [13] Roque Corral, Antonio Escribano, Fernando Gisbert, Adolfo Serrano, and Carlos Vasco. chapter Validation of a Linear Multigrid Accelerated Unstructured Navier-Stokes Solver for the Computation of Turbine Blades on Hybrid Grids. *Aeroacoustics Conferences*. American Institute of Aeronautics and Astronautics, May 2003.

- [14] Jose Ramon Fernandez Aparicio, Adolfo Serrano, and Raul Vazquez. chapter On the Linearity of Turbomachinery Interaction Noise. Part I: 2D Analysis. Aeroacoustics Conferences. American Institute of Aeronautics and Astronautics, Jun 2011.
- [15] Jose Ramon Fernandez Aparicio, Adolfo Serrano, and Raul Vazquez. chapter On the Linearity of Turbomachinery Interaction Noise. Part II: 3D Analysis. Aeroacoustics Conferences. American Institute of Aeronautics and Astronautics, Jun 2012.
- [16] Adolfo Serrano Gonzalez and Jose Ramon Fernandez Aparicio. Turbine tone noise prediction using a linearized cfd solver: Comparison with measurements, 2015.
- [17] Thomas Law, Roque Corral, Jose Ramon Fernandez Aparicio, and Adolfo Serrano. chapter Linear Viscous Eigenmode Analysis Within a Radially Varying Swirling Flow. Aeroacoustics Conferences. American Institute of Aeronautics and Astronautics, Jun 2010.
- [18] V. V. Golubev and H. M. Atassi. Acoustic-vorticity waves in swirling flows. *Journal of Sound and Vibration*, 209(2):203–222, 1998.
- [19] Pierre Moinier, Michael Giles, and John Coupland. Three-dimensional nonreflecting boundary conditions for swirling flow in turbomachinery. *Journal of Propulsion and Power*, 23(5):981–986, Sep 2007.